Synthesis and crystallographic study of cation substituted NZP materials: $Na_{1+x}Zr_{2-x}M_xP_3O_{12}$ (M = Sb, Al, Cr and x = 0.1)

Rashmi Chourasia, and O. P. Shrivastava[a)]
Department of Chemistry, Dr. H.S. Gour University, Sagar 470 003, India

(Received 28 February 2013; accepted 28 February 2013)

A novel concept of immobilization of light water nuclear reactor fuel reprocessing waste effluent through interaction with sodium zirconium phosphate (NZP) has been established. It was found that a large number of hazardous cations could be loaded in the NZP-based matrix without significant change of three-dimensional framework structure. Starting from the raw powder diffraction data of polycrystalline solid phases, crystal structure of substituted NZP phases has been investigated using the General Structure Analysis System (GSAS) package. Cation(s) substituted NZP phases crystallize in rhombohedral symmetry (space group *R*-3*c* and $Z = 6$). Powder diffraction data have been subjected to Rietveld refinement to reach satisfactory structural convergence of *R*-factors. Unit cell parameters, inter atomic distances, bond angles, reflecting planes (h, k, l), structure factors, polyhedral (ZrO_6 and PO_4) distortion, and particle size have been reported. PO_4 stretching and bending vibrations in the Infra red (IR) region have been assigned. SEM and EDAX analysis provide analytical evidence of fixation of cations in the matrix. © *2013 International Centre for Diffraction Data.*
[doi:10.1017/S0885715613000183]

Key words: sodium zirconium phosphate, X-ray powder diffraction, Rietveld refinement, SEM, EDX

I. INTRODUCTION

The general crystallochemical formula for sodium zirconium phosphate (NZP) group of materials is described as $(M_1)\ (M_2)_3\ \{[L_2\ (PO_4)_3]^{\ P-}\}_{3\infty}$ where M_1 and M_2 are crystallographic positions in the framework holes and L the positions of the framework. The NZP core framework and the ions placed into M_1 and M_2 sites behave as two parts of the structure playing different roles. Bonds between the atoms of the framework are strongly covalent, whereas the inserted ions to M_1 and M_2 interstitial sites are relatively weakly bonded. The weakest one is for cations like Na having +1 oxidation state. This combination of stability and flexibility of NZP structure allows the existence of iso and heterovalent substitutions at all non-oxygen lattice sites and gives rise to a large number of compounds with identical connections between their structural units (Petkov *et al.*, 2001). Based on the available coordination sites, the standard structural formula for such compounds is described as $[M']\ [M''_3]\ [A_2^{VI}]\ [X_3^{IV}]\ O_{12}$. The octahedral site $A^{\mathbf{VI}}$ is normally occupied by Zr^{4+} while the $X^{\mathbf{IV}}$ site is tetrahedral and occupied by P^{5+}. In rhombohedral polycrystalline sodium zirconium phosphates, the PO_4 tetrahedra are linked with ZrO_6 octahedra by corner sharing, hence forming a three-dimensional framework with $[Zr_2(PO_4)_3]^-$ where each oxygen atom is bonded to only one P and one Zr atom. The columns of three units lie along the **c**-direction running in hexagonal unit cell parallel to each other. These columns are inter-linked through PO_4 tetrahedra in the direction perpendicular to the **c**-axis to develop a framework of columns, which are capable of accommodating the larger alkali metal cations. The three-dimensional NZP structure possesses two kinds of holes, site I (M'_1) occurs in the column of Zr octahedra and the other site II (M''_2) is located between columns of Zr octahedra. This M''_2 site can be populated by additional cations that compensate the charge with polyvalent cations other than zirconium in the three-dimensionally linked interstitial spaces. The alkali atoms such as Na, K, Ca, Ba, Mg, and Sr etc. can be located in the holes between ZrO_6 octahedra (Yoon *et al.*, 2001). Site I has distorted octahedral coordination, while site II has trigonal prismatic coordination (Bhuvneshwari and Varadaraju, 1999; Bois *et al.*, 2001). Several divalent cations substitute for two alkali ions, while rare earth elements are assumed to occupy the Zr^{4+} site. The strongly bonded but open NZP structure allows high mobility of alkali ions tunneling through the PO_4–ZrO_6 polyhedral chain. As a result, there are a number of compounds containing 1–5 different cations, belonging to this family (Rega *et al.*, 1992; Varadaraju *et al.*, 1994; Petkov and Orlova, 2003). They are also well known for their applications as catalyst supporters, fast ion conductors, and host for immobilizing radioactive waste effluents (Breval *et al.*, 1998; Tantri *et al.*, 2002). This communication describes the synthesis and Rietveld refinement of crystal structures of trivalent substituted NZP phases.

II. EXPERIMENTAL

The stoichiometric amount of AR grade Na_2CO_3, ZrO_2, Sb_2O_3/ Cr_2O_3/Al_2O_3, and $NH_4H_2PO_4$ were mixed in a mortar and pestle with an appropriate quantity of glycerol to make a semisolid paste. The paste was gradually heated initially at 600 °C for 8 h to decompose Na_2CO_3 and $(NH_4)H_2PO_4$ with the emission of carbon dioxide, ammonia and water

[a)]Author to whom correspondence should be addressed. Electronic mail: dr_ops11@rediffmail.com

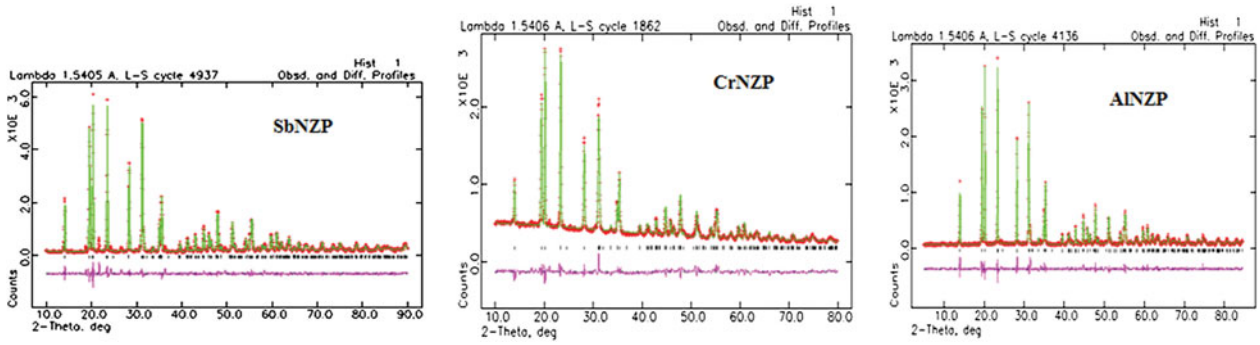

Figure 1. Rietveld refinement patterns of SbNZP, CrNZP, and AlNZP ceramic samples. The ' + ' are the raw XRD data and the overlapping continuous line is the calculated pattern. Black vertical lines in the profile indicate Bragg's positions of allowed reflections for Cu$K\alpha$1 and Cu$K\alpha$2. The curve at the bottom is the difference in the observed and calculated intensities in the same scale.

vapor. The mixture was reground to micron size, pressed into pellet at room temperature and finally sintered in a platinum crucible at 1050 °C for 24 h.

The materials were characterized by powder X-ray diffraction (XRD) between $2\theta = 10$–$90°$ on a Rigaku RUH3R diffractometer using Cu$K\alpha$ radiation at a step size of $2\theta = 0.02°$ and a fixed counting rate of 2 s per step. The data were analyzed by the Rietveld method using the General Structure Analysis System (GSAS), which is capable of handling and refining the step analysis diffraction data in a comprehensive manner. SEM and EDAX analysis of antimony, chromium, and aluminum substituted NZP has been performed on JEOL JSM-5600 microscope.

III. RESULTS AND DISCUSSION

Phase pure solid solutions of SbNZP, CrNZP, and AlNZP crystallize in the rhombohedral system (space group *R*-3*c*). The conditions for the rhombohedral lattice: (i) $-h + k + l = 3n$, (ii) when $h = 0$, $l = 2n$, and (iii) when $k = 0$, $l = 2n$ have been verified for reflections between $2\theta = 10$–$90°$. The intensity and positions of the diffraction patterns match with the characteristic pattern of sodium zirconium phosphate, which give several prominent reflections between $2\theta = 13.98$–$46.47°$ [JCPDS file no. 71-0959 (2000; Figure 1]. The Rietveld refinement of all three phases was performed by the least squares method using GSAS software (Larson and Von Dreele, 2000). Assuming that $Na_{1.1}Zr_{1.9}Sb_{0.1}P_3O_{12}$, $Na_{1.1}Zr_{1.9}Al_{0.1}P_3O_{12}$, and $Na_{1.1}Zr_{1.9}Cr_{0.1}P_3O_{12}$ belong to the Nasicon family, Zr, P, and O atoms are in the 12*c*, 18*e*, and 36*f* Wyckoff positions, respectively, of the *R*-3*c* space group. The Na atoms were assumed to occupy the M_1 and M_2 sites. In the first step, Na occupies fully the M_1 site (6*b*) and the excess of sodium was located in the M_2 site (18*e*). In the second step, the occupancies of Na1 and Na2 were allowed to vary, but the total Zr and Sb/Al/Cr contents were constrained to 0.95 and 0.05, respectively. The refinement leads to a rather good agreement between the experimental and calculated diffraction pattern and yields acceptable reliability factors (R_p, R_{wp} and RF^2). The normal probability plot for the histogram gives nearly a linear relationship indicating that the *Io* and *Ic* values for most part of the curve are normally distributed. The unit-cell parameters of the materials are close to the corresponding values for un-substituted NZP (Carla *et al.*, 1997). The unit-cell parameters register slight increase in the ***c***-direction (Table I). The presence of $Na(1)O_6/Na(2)O_8$ distorted polyhedron in the M_2 site stretches the bridging PO_4 tetrahedra in the ***c***-direction. Simultaneously, the structures show a slight contraction along the ***a***-direction. This may be attributed to bond-angle distortions as a result of the coupled rotation of ZrO_6 and PO_4 polyhedra (Govindan Kutty *et al.*, 1998).

Alteration in unit-cell parameters indicates that the network slightly modifies its dimensions to accommodate the

TABLE I. Crystallographic data for SbNZP, CrNZP, and AlNZP ceramic phases at room temperature.
Structure: rhombohedral; space group; R-3c; Z = 6.

Parameter	SbNZP	CrNZP	AlNZP
Unit-cell parameters			
a(Å)	8.772 83(16)	8.787 36(19)	8.797 01(16)
b(Å)	8.772 83	8.787 36	8.797 01
c(Å)	22.8375(7)	22.7461	22.7700(7)
$A = \beta = 90.0°$, $\gamma = 120.0°$			
R_p	0.0764	0.0375	0.0936
R_{wp}	0.1099	0.0492	0.1288
$R_{expected}$	0.0547	0.0485	0.0842
RF^2	0.045 00	0.167 34	0.0570
Volume of unit cell (Å^3)	1522.16(4)	1521.09(6)	1526.04(5)
S (GoF)	2.02	1.01	1.53
Unit cell formula weight	3036.666	2932.700	2916.0
Density$_{X\text{-}ray}$ (g/cm^3)	3.313	3.173	3.202
Slope	1.6688	0.9148	

TABLE II. Atom-oxygen bond distances (Å) of SbNZP, CrNZP, and AlNZP ceramic powders at room temperature.

Na1–O7	2.590 00(5) × 6	2.547 28(7) × 6	2.550 01(5) × 6
Na2–O6	2.865 31(5) × 2	2.327 11(7)	2.329 60(5)
Na2–O6	2.815 44(5) × 2	2.512 35(5)	2.515 10(4)
Na2–O7	2.466 04(4)	2.694 57(6)	2.697 53(5)
Na2–O7	2.395 14(4)	2.736 18(6)	2.739 18(5)
Na2–O7	2.466 04(4)	2.435 49(5)	2.438 16(4)
Na2–O7	2.395 14(4)	2.202 16(4)	2.204 57(4)
Zr3/M–O6	2.027 14(30) × 3	2.047 78(4) × 3	2.054 92(3) × 3
Zr3/M–O7	2.066 47(30) × 3	2.075 21(5) × 3	2.071 77(3) × 3
P5–O6	1.521 930(30) × 2	1.517 70(5) × 2	1.519 32(3) × 2
P5–O7	1.533 950(30) × 2	1.552 53(3) × 2	1.554 23(3) × 2

https://doi.org/10.1017/S0885715613000183 Published online by Cambridge University Press

TABLE III. O–M–O angles (degree) in SbNZP, CrNZP, and AlNZP ceramic powders at room temperature.

Angles (°)	SbNZP	CrNZP	AlNZP
O7–Na1–O7	65.0877(16) × 6,180.0 × 3, 114.9123(16) × 6	65.567(2) × 6,180.0 × 3, 114.433(2) × 6	65.569(2) × 6,180.0 × 3, 114.431(2) × 6
O6–Na2–O7	69.9337 × 2, 130.4187 × 2, 60.5637, 159.6394	61.382(1), 106.607(1) 145.116, 168.530,107.761, 71.853(2),71.249(1) 131.943,	61.381(1), 106.606(1), 145.116, 168.530,107.761, 71.851(1), 71.249(1) 131.943,
O6–Na2–O7		103.005(2),	103.006(2),
O7–Na2–O7		141.334(1), 128.530(1)	141.335(1), 128.531(1)
		61.048,72.801,59.405, 117.164(1)	61.048, 72.802,59.405, 117.164
O6–Zr3–O6	90.700 08(14) × 3	92.446(2) × 3	
O7–Zr3–O7	84.7889(15) × 3	83.309(2) × 3	83.591(2) × 3
O6–Zr3–O7	92.3189(14) × 3, 175.8893 × 3, 92.050(14) × 3	91.822(2) × 3,92.446(2) 173.639 × 3,92.083(2) × 3	91.844(1) × 3,92.162(1) 174.034 × 3,92.104(1) × 3
O6–P5–O6	109.3417(19)	112.016(2)	112.014(2)
O7–P5-O7	108.3209	110.540	110.540
O6–P5–O7	107.669 20(10) × 2, 111.9412(8) × 2	113.171(1) × 2,104.095 × 2 112.016(2)	113.172(1) × 2,104.096 × 2 112.014(2)

cations occupying M_1 and M_2 sites without breaking the bonds. The basic framework of NZP accepts the cations of different sizes and oxidation states to form solid solutions yet at the same time keeping the overall geometry unchanged. The final atomic coordinates, inter-atomic distances (Table II), bond angles (Table III), and (*h k l*) values corresponding to prominent reflections are extracted from the crystal information file (CIF) prepared by the software. The refinement leads to acceptable Zr/M–O, P–O, and Na–O bond distances (where M = Sb, Cr and Al) Zr/M atoms are displaced from the center of the octahedron because of the Na^+–Zr^{4+}/M^{3+} repulsions. The average Zr/M–O distance 2.0468 Å for SbNZP, 2.0615 Å for CrNZP, and 2.0633 Å for AlNZP is smaller than the values calculated from the ionic radii data of 2.12 Å (Shannon, 1976). The P–O distances are close to those found in Nasicon-type phosphates (Chakir *et al.*, 2006). The O–(Zr/M)–O angles vary between 83.31and 175.89°, the angles implying shorter bonds are superior to those involving longer ones because of O–O repulsions which are stronger for O(6)–O(6) than for O(6)–O(7).

The O–P–O angles vary from 104.09 to 113.17°. The Na (1) atoms occupy the center of the M_1 site, while Na(2) atoms located in the M_2 site are surrounded by eight or six oxygen atoms. Figure 2 shows the PLATON projection of the molecular structure depicting the inter linking of ZrO_6 and PO_4 through a bridge oxygen atom. The ORTEP view generated by the refined structural data shows that the Zr–O bonds are in three pairs resulting in six coordinations of zirconium and P–O distanced in one pair resulting in four coordinations of phosphorus. Figure 3 illustrates the DIAMOND view showing the ZrO_6 inter ribbon distance in the structure of the title phase which is a function of amount and size of alkali cation in the M(2) site of the 3D framework, built from ZrO_6 octahedra and corner sharing PO_4 tetrahedra. The bond valences calculated using valence sum rule (West, 2003) are in agreement with the expected formal oxidation states of Na^+, Zr^{4+}, and P^{5+}, respectively. The chemical bonding mechanism based on the contour maps of charge density reveals that at the center of the Zr atoms the charge density maxima are between 5.75 and 5.82 a.u.^{3}. There are two charge density minima for two different bond distances between Zr and O atoms. The Zr–O bond is covalent with some degree of ionic character because of hybridization effect between Zr-4d and O-2p states (Terki

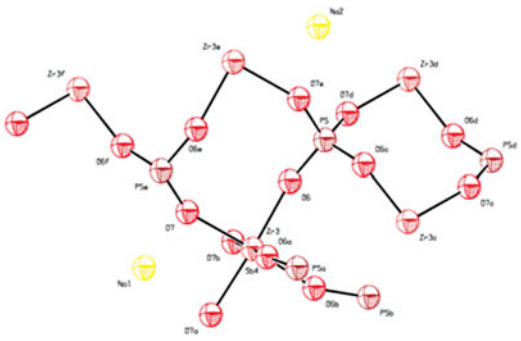

Figure 2. PLATON projection of molecular structure showing Zr coordination in ZrO_6 and P coordination in PO_4 polyhedron at 50% probability level.

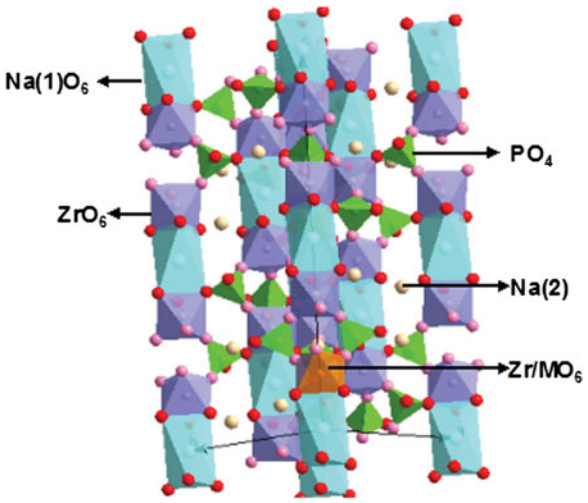

Figure 3. DIAMOND view of coordination sites of Na, Zr/M, (Sb, Cr, Al) and P.

https://doi.org/10.1017/S0885715613000183 Published online by Cambridge University Press

TABLE IV. Bond distortions in ZrO_6, $Na(2)O_8$, and PO_4 structural units of SbNZP, CrNZP, and AlNZP ceramic sample.

Polyhedral distortion (Å)			
Polyhedron	NZPSb	NZPCr	NZPAl
ZrO_6	0.923×10^{-4}	0.44×10^{-4}	0.167×10^{-4}
NaO_6/NaO_8	61.79×10^{-4}	58.08×10^{-4}	58.09×10^{-4}
PO_4	0.155×10^{-4}	1.286×10^{-4}	1.29×10^{-4}

et al., 2005), Similarly, there are two electron density minima for two types of P–O bond lengths 1.5219(30) and 1.5339(30) Å, respectively. The charge density ratios at the center of the Zr and P atoms of various contours vary from a low of 3.01 to a high of 4.36 against the expected value of 3.6.

From the individual bond lengths of metal-oxygen polyhedra, polyhedral distortion can be calculated by the following equation $\Delta = 1/n\ \Sigma\{(R_i - R_m)/(R_m)\}^2$ (Roger *et al.*, 2004). The calculated distortions in ZrO_6 octahedra, PO_4 tetrahedra, and

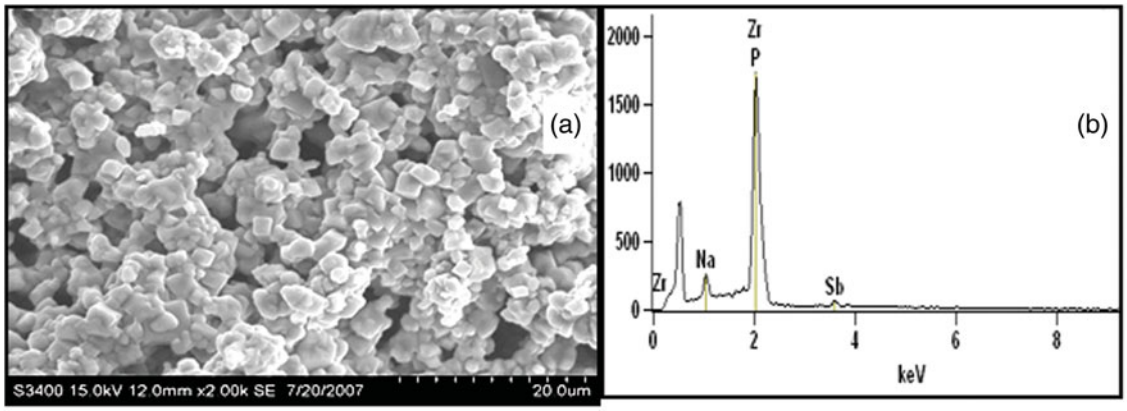

Figure 4. (a) Scanning electron micrograph and (b) EDAX spectrum of polycrystalline SbNZP mono phase.

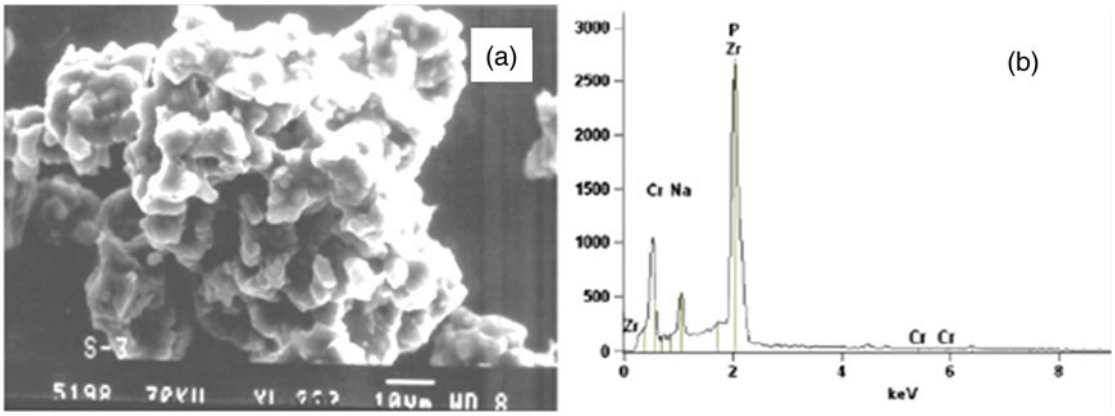

Figure 5. (a) SEM and (b) EDAX spectrum of CrNZP ceramic powder synthesized at 1050 °C.

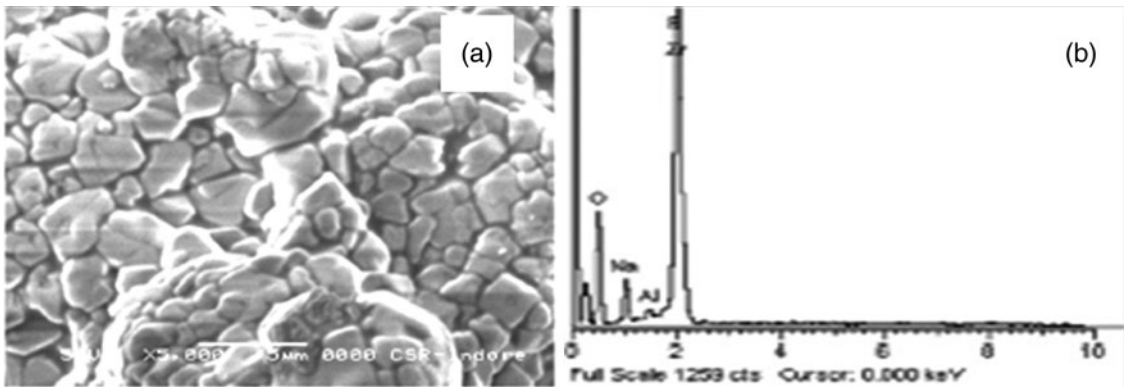

Figure 6. (a) SEM and (b) EDAX spectrum of AlNZP ceramic material synthesized at 1050 °C.

https://doi.org/10.1017/S0885715613000183 Published online by Cambridge University Press

NaO_8 polyhedra have been summarized in Table IV. The ZrO_6 octahedron of Al-substituted NZP has been found to be approximately three times more distorted than the corresponding octahedron of Cr-substituted NZP.

The morphology and microstructure of the specimen have been examined by scanning electron microscopy. The evolution of solid monophase is seen clearly in the electron micrographs of ceramic powders, Sb-substituted NZP has parallelepiped grains 1.5–2.0 μm in diameter [Figure 4(a)], Cr and Al-substituted NZP phases show isolated grains of approximately 2.5–3.0 μm visible in the form of their agglomerates [Figures 5(a) and 6(a)]. The EDX analysis of the phases on selected locations on atomic and weight % of Na, Zr, Sb/Al/Cr, and P are acceptable with their corresponding expected molar ratios. The EDX spectrum reveals that antimony/chromium/aluminum is crystallochemically fixed in the NZP matrix [Figures 4(b), 5(b), and 6(b)]. Simultaneously, the crystallite size was also studied using Scherrer's equation where broadening of the peak is expressed as full-width at half-maxima (FWHM) in the recorded XRD pattern (Shrivastava and Chourasia, 2008). The crystallite size measured along various reflecting planes does not show significant *h. k. l* dependent broadening; however, the minimum and maximum size depends on substituent cation (Sb, Cr, and Al).

ACKNOWLEDGEMENTS

The authors thankfully acknowledge the financial assistance received from the Department of Science and Technology, Government of India, New Delhi for research project no. SR/S3/ME/20/2005-SERC-Engg. under the SERC scheme. Rashmi Chourasia is thankful to UGC, New Delhi, India for the award of Dr D.S. Kothari Post Doctoral fellowship (PDF).

Bhuvneshwari, G. and Varadaraju, U. V. (**1999**). "Synthesis of new network phosphates with NZP structure," J. Solid State Chem. **145**, 227.

Bois, L., Guitter, M. J., Carrot, F., Trocellier, P., and Guatier-Soyer, M. (**2001**). "Preliminary results on the leaching process of phosphate ceramics, potential hosts for actinide immobilization," J. Nucl. Mater. **297**, 129–137.

Breval, E., McKinstry, H. A., and Agrawal, D. K. (**1998**). "Synthesis and thermal expansion properties of the $Ca_{(1+x)/2}Sr_{(1+x)/2}Zr_4P_{6-2x}Si_{2x}O_{24}$ system," J. Am. Ceram. Soc. **81**, 962–1032.

Carla, V., Garrido, F. M., Alves, O. L., Calle, P., Martinez Juarez, A., Iglesias, J. E., and Rojo, J. M. (**1997**). "Ionic conductivity and structural characterization of $Na_{1.5}Nb_{0.3}Zr_{1.5}(PO_4)_3$ with NASICON-type structure," Solid State Ion. **100**, 127–134.

Chakir, M., El Jazouli, A., and de Waal, D. (**2006**). "Synthesis, crystal structure and spectroscopy properties of $Na_3AZr(PO_4)_3$ (A: Mg, Ni) and $Li_{2.6}Na_{0.4}NiZr(PO_4)_3$ phosphates," J. Solid State Chem. **179**, 1883–1891.

Govindan Kutty, K. V., Asuvathraman, R., and Sridharan, R. (**1998**). "Thermal expansion studies on the sodium zirconium phosphate family of compounds $A_{1/2}M_2(PO_4)_3$: effect of interstitial and framework cations," J. Mater. Sci. **33**, 4007–4013.

JCPDS Powder Diffraction Data File No. 71-0959. (**2000**). Compiled by International Center for Diffraction Data U.S.A.

Larson, A. C. and Von Dreele, R. B. (**2000**). General Structure Analysis System Technical Manual LANSCE, MS-H805, Los Alamos National University LAUR, 86–748.

Petkov, V. I. and Orlova, A. I. (**2003**). "Crystal-chemical approach to predicting the thermal expansion of compounds in the NZP family," Inorg. Mater. **39**, 1013–1023.

Petkov, V. I., Orlova, A. I., Kazantsev, G. N., Samoilov, S. G., and Spiridonova, M. L. (**2001**). "Thermal expansion in the Zr and 1-, 2-valent complex phosphates of NaZr2(PO4)3 (NZP)," J. Thermal Anal. Calor. **66**, 623–632.

Rega, D. A., Agrawal, D. K., Huang, C. Y., and McKinstry, H. A. (**1992**). "Microstructure and microcracking behavior of barium zirconium phosphate ($BaZr_4P_6O_{24}$) ceramics," J. Mater. Sci. **27**, 2406–2412.

Roger, H. M., Ruslan, P., and Liferovich, A. (**2004**). "Structural study of the perovskite series $Ca_{1-x}Na_xTi_{1-x}Ta_xO_3$," J. Solid State Chem. **177**, 4420–4427.

Shannon, R. D. (**1976**). "Effective ionic radii in oxides and fluorides," Acta Crystallogr. A **32**, 751.

Shrivastava, O. P. and Chourasia, R. (**2008**). "Crystal chemistry of sodium zirconium phosphate based simulated ceramic waste forms of effluent cations (Ba^{2+}, Sn^{4+}, Fe^{3+}, Cr^{3+}, Ni^{2+} and Si^{4+}) from light water reactor fuel reprocessing plants," J. Hazard. Mater. **153**, 285–292.

Tantri, S., Ushadevi, S., and Ramasesha, S. K. (**2002**). "High temperature X-ray studies on barium and strontium zirconium phosphate based low thermal expansion materials," Mater. Res. Bull. **37**, 1141–1147.

Terki, R., Bertrand, G., and Aourag, H. (**2005**). "The proceedings of the 2nd international symposium on nano and giga-challenges in microelectronics," Microelectron. Eng. **81**, 514–523.

Varadaraju, M., Sugantha, U. V., and Subba Rao, G. V. (**1994**). "Synthesis and characterization of NZP phases, $AM^{'3+}M^{''4+}P_3O_{12}$," J. Solid State Chem. **111**, 33–40.

West, A. R. (**2003**). *Solid State Chemistry and its Application* (John Willey and Sons, Singapore), chapter A9, pp. 710.

Yoon, C. S., Kim, J. H., Kim, C. K., and Hong, K. S. (**2001**). "Synthesis of low thermal expansion ceramics based on $CaZr_4(PO_4)_6$–Li_2O system," Mater. Sci. Eng. B **79**, 6–10.